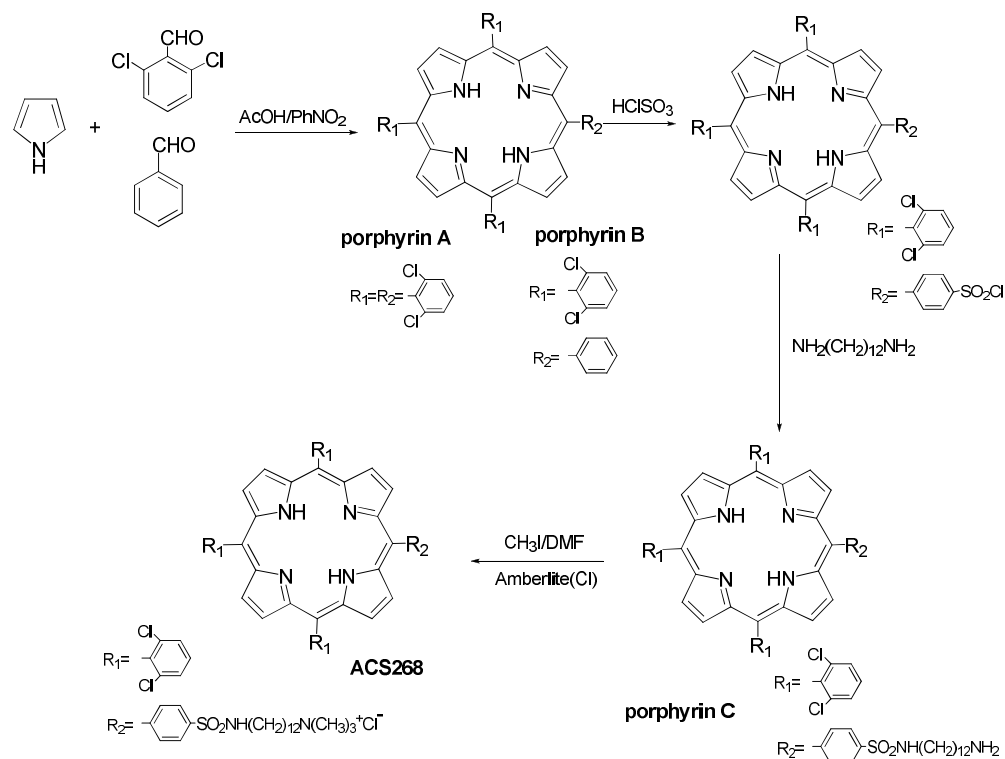


Supplementary Information

Synthesis of ACS268

The synthesis of ACS268 is outlined in Scheme S1.

Scheme S1



To a solution of 2,6-dichlorobenzaldehyde (7.0 g, 40 mmol) and benzaldehyde (0.85 g, 8.0 mmol) in acetic acid (100 mL), acetic anhydride (8 mL) and nitrobenzene (25 mL) at 120 °C, pyrrole (3.5 mL, 50 mmol) was added. The reaction mixture was maintained at this temperature for 2 hours. After cooling, a mixture (275 mg) of 5-phenyl-10,15,20-*tris*(2,6-dichlorophenyl)porphyrin (A) and tetrakis(2,6-dichlorophenyl)porphyrin (B) was obtained.

Synthesis of 5,10,15-tris(2,6-dichlorophenyl)-20-[N-(12-amino-dodecyl-p-sulphonamidophenyl)]porphyrin (porphyrin C). At room temperature, chlorosulfonic acid (20 mL) was added to the mixture of porphyrin A and B (250 mg). The solution was stirred for 2 h and then carefully poured over ice in order to precipitate the chlorosulphonyl derivative of porphyrin B and unreacted porphyrin A, which does not react at this temperature due to ring deactivation. The precipitate was filtered, dried, dissolved with chloroform and the solution dried with sodium sulphate (Na_2SO_4). The solution was concentrated to 30 mL and was added to 1,12-diaminedodecane (0.8 g) and pyridine (2 mL). The mixture was stirred overnight at 30 °C and filtered. After concentration the residue was chromatographed on silica gel type 60 with particle size of 0.035–0.070 μm (Acros Organics, **city, country**). The porphyrin fraction was eluted first with dichloromethane and then dichloromethane/ethyl acetate/ethanol (70/30/10). Evaporation of the solvent generated 120 mg of porphyrin C [MS (ESI): m/z 1083 (100%, $[\text{M}+1]^+$).

Synthesis of 5,10,15-tris(2,6-dichlorophenyl)-20-[N-(12-trimethyl ammonium chloride)-dodecyl-p-sulphonamidophenyl]porphyrin (ACS268). Porphyrin C (100 mg) was dissolved in DMF (1 mL) and 2 methyl iodide (2 mL) and K₂CO₃ (150 mg) were added. The solution was stirred for 24 h at 60 °C in a sealed tube and, after cooling, was poured over ice water to precipitate. The solid was filtered, dissolved in dichloromethane and dried over Na₂SO₄. Then, the solution was concentrated to 10 mL, stirred for 30 min. with Amberlite 400 (Cl form), filtered and washed with methanol. Evaporation of the solvent gave a solid which was recrystallized (CH₂Cl₂/hexane) to afford 70 mg of ACS268. δ_{H} (400 MHz, *d*₆-DMSO) 8.75 (m, 8H, β -H), 8.47 (d, 2H, *J* = 7.2 ArH), 8.23 (d, *J* = 7.2 Hz, 2H, Ar-H), 8.03-7.96 (m, 9H, Ar-H), 3.12-2.90 (m, 13H, (CH₃)₃,CH₂N), 1.25 (m, 20H, CH₂), HRMS (ESI): *m/z* calc. for C₅₉H₅₇Cl₆N₆O₂S (M⁺) 1123.23778; found, 1123.23894.

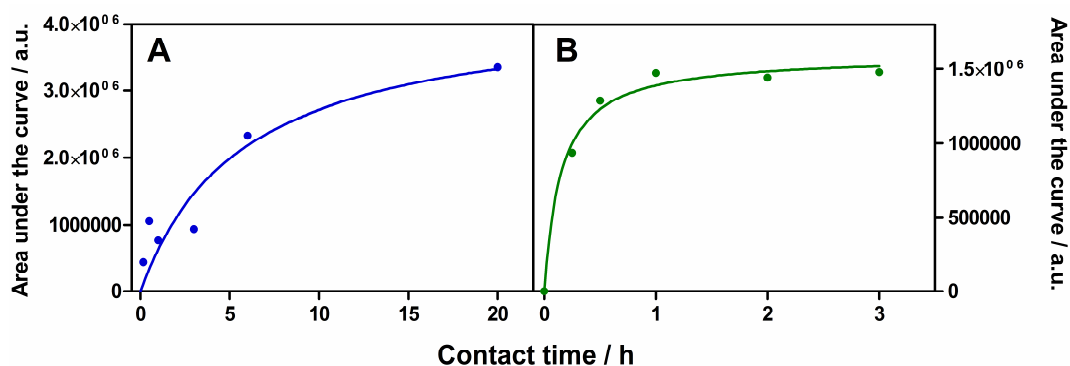
Control measurements in bacterial suspensions

- 1) Origin of the luminescence signals: It was critical in our experiments to eliminate any PS molecule from the external aqueous buffer in order to ensure that the observed fluorescence or phosphorescence was produced by cell-bound molecules only. The external aqueous solutions were routinely tested before and after the *in vitro* measurements.
- 2) Light dose: Irradiation during APDT may induce the release or relocalization of the PS from its initial binding site [1]. Also, the kinetics of ¹O₂ formation and decay may change upon irradiation due to the photodynamic modification of cell components [2,3]. In order to prevent these effects, all the experiments were performed with the lowest possible amount of energy per bacterial cell (7 nJ/cell), well below the doses reported by Kuimova *et al.* [2] in eukaryotic cells (*ca.* 0.5 mJ/cell) and comparable to those used by Schlothauer *et al.* (2-40 nJ/cell) [3].
- 3) Identification of ¹O₂ as the species responsible for the emission recorded at 1,270 nm: Many controls have been carried out to demonstrate that we were indeed looking at ¹O₂ in the luminescence experiments with *E. coli*:
 - No signal could be detected in the absence of PS.
 - No signal was observed at 1150 nm under any conditions, i.e., the spectrum of the signal matched that of ¹O₂ [4].
 - The phosphorescence disappeared when oxygen was excluded from the medium by flowing a stream of argon above the cell suspension for 1 h.
 - The duration of the luminescence increased when H₂O was replaced by D₂O in the buffer.

PS binding to *E.coli*

We investigated the uptake of NMB and ZnTMPyPz (Figure S1) at contact times higher than the typical ones used in antimicrobial photodynamic therapy (APDT) in order to attain a cellular concentration high enough to allow our measurements. To eliminate any non-bound molecule, the uptake was measured after three rounds of cell centrifugation, washing, and resuspension in buffer. This procedure also eliminates any molecules that leaked from the cells [5].

Figure S1. *E. coli* uptake of (A) NMB and (B) ACS268, with a bulk concentration of 10 μ M and 7.5 μ M, respectively.



Time-resolved fluorescence measurements

The time-resolved fluorescence decays were measured for NMB and ZnTMPyPz.

Figure S2. Time-resolved fluorescence of NMB at 657 nm upon excitation at 596 nm. Signal, instrument response function, and fit in (A) PBS at pH 7.4, and (B) *E. coli*.

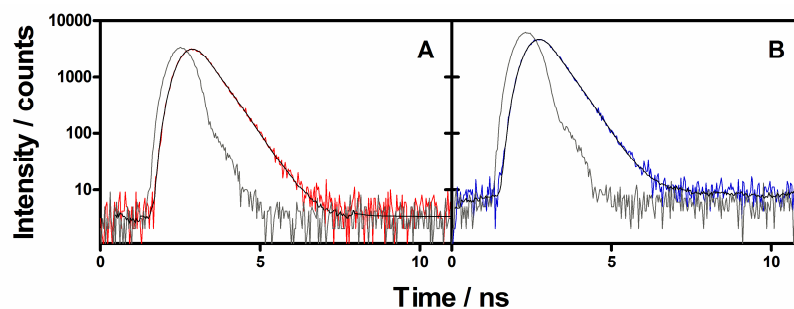
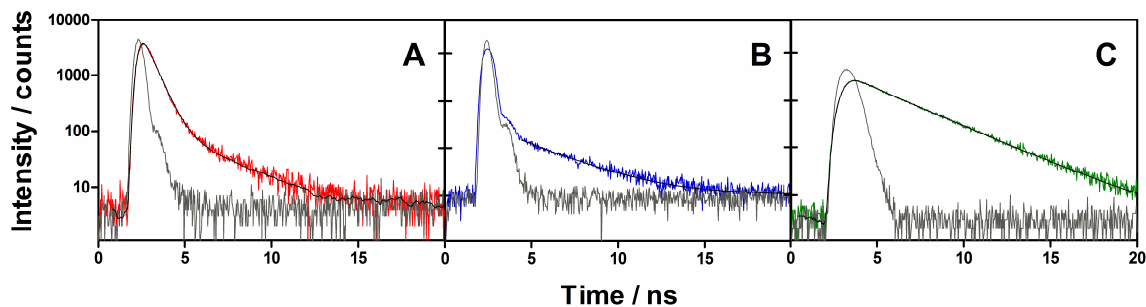
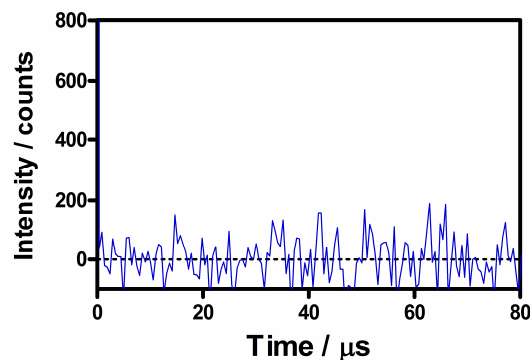


Figure S3. Time-resolved fluorescence of ZnTMPyPz at 675 nm upon excitation at 596 nm. Signal, instrument response function, and fit in (A) PBS at pH 7.4, (B) *E. coli*, and (C) DMF.



Singlet oxygen in *E. coli* photosensitised by ZnTMPyPz

Figure S4. Singlet oxygen phosphorescence at 1270 nm using ZnTMPyPz as photosensitiser in *E. coli* cells suspended in D-PBS.



Singlet oxygen quantum yield of ACS268 in solution

The quantum yield of singlet oxygen production (Φ_{Δ}) is defined as the number of photosensitized $^1\text{O}_2$ molecules per absorbed photon.

The quantum yields of $^1\text{O}_2$ production were determined by comparing the amplitude of the signal of ACS268 to that produced by an optically matched solution of phenalenone as reference ($\Phi_{\Delta}^{\text{PN}} = 0.85$ in DMA [6], assumed to hold in DMF; $\Phi_{\Delta}^{\text{TMPyP}} = 0.75$ in D_2O [7]) in the same solvent and at the same excitation wavelength and intensity (Eq. S1).

The Φ_{Δ} value in D_2O was measured in a 99.7:0.3 mixture of D_2O :DMF necessary to solve the product.

$$\Phi_{\Delta}(\text{sample}) = \frac{A_{\text{sample}}}{A_{\text{ref}}} \cdot \Phi_{\Delta}(\text{ref}) \quad (\text{S1})$$

Figure S5. (A) Absorption spectra of optically matched solutions at 355 nm of ACS268 (red) and phenalenone (blue) in DMF. **(B)** $^1\text{O}_2$ phosphorescence signals at 1270 nm of ACS268 (red) and phenalenone (blue) in DMF upon irradiation at 355 nm.

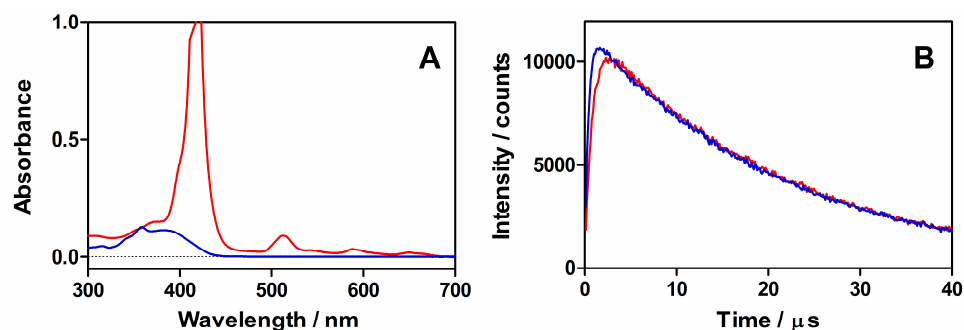
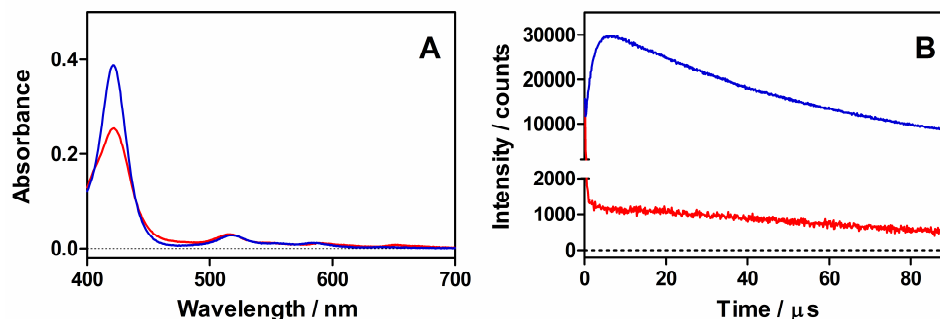


Figure S6. (A) Absorption spectra of optically matched solutions at 532 nm of ACS268 (red) and TMPyP (blue) in D₂O. (B) ¹O₂ phosphorescence signals at 1270 nm of ACS268 (red) and phenaleneone (blue) in D₂O upon irradiation at 532 nm.

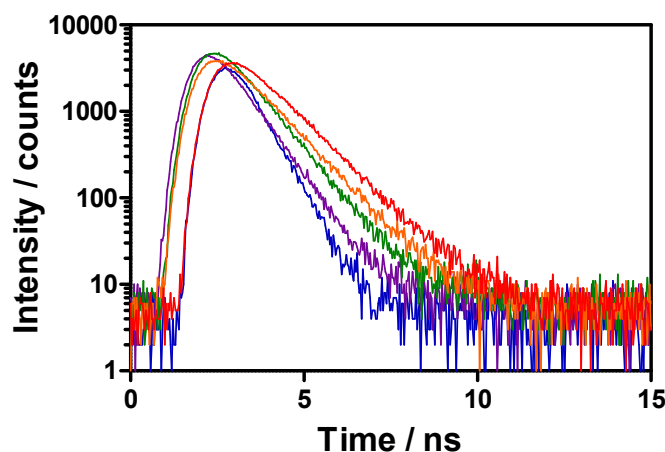


Thus, a Φ_{Δ} of 0.87 ± 0.01 and 0.04 ± 0.01 is calculated for ACS268 in DMF and D₂O, respectively.

Solvent polarity dependence of the fluorescence intensity of NMB

The fluorescence lifetime of 1 μ M solutions of NMB in different solvents with increasing polarities show a clear dependence as demonstrated in Fig. S7.

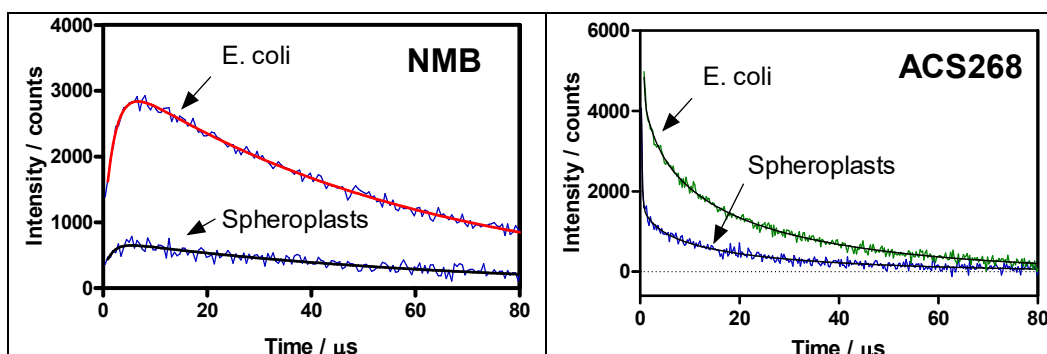
Figure S7. Time-resolved fluorescence decay of NMB at 657 nm upon excitation at 596 nm in H₂O (0.5 ns; blue), MeOH (0.7 ns; violet), EtOH (0.8 ns; green), 1-pentanol (1.0 ns; orange) and 1-hexanol (1.1 ns; red).



Singlet oxygen phosphorescence in spheroplasts

The kinetics of singlet oxygen phosphorescence of NMB and ACS268 in spheroplasts is substantially weaker than in intact cells, which indicates that these dyes are localized in the cell wall

Figure S8. Time-resolved $^1\text{O}_2$ phosphorescence signals at 1270 nm for NMB and ACS268 in intact *E. coli* cells and the corresponding spheroplasts.



References

- Jori, G.; Fabris, C.; Soncin, M.; Ferro, S.; Coppellotti, O.; Dei, D.; Fantetti, L.; Chiti, G.; Roncucci, G. Photodynamic therapy in the treatment of microbial infections: Basic principles and perspective applications. *Lasers Surg. Med.* **2006**, *38*, 468–481.
- Kuimova, M.K.; Botchway, S.W.; Parker, A.W.; Balaz, M.; Collins, H.A.; Anderson, H.L.; Suhling, K.; Ogilby, P.R. Imaging intracellular viscosity of a single cell during photoinduced cell death. *Nat. Chem.* **2009**, *1*, 69–73.
- Schlothauer, J.; Hackbarth, S.; Roder, B. A new benchmark for time-resolved detection of singlet oxygen luminescence—Revealing the evolution of lifetime in living cells with low dose illumination. *Laser Phys. Lett.* **2009**, *6*, 216–221.
- Schweitzer, C.; Schmidt, R. Physical mechanisms of generation and deactivation of singlet oxygen. *Chem. Rev.* **2003**, *103*, 1685–1757.
- Reddi, E.; Cecon, M.; Valduga, G.; Jori, G.; Bommer, J.C.; Elisei, F.; Latterini, L.; Mazzucato, U. Photophysical properties and antibacterial activity of meso-substituted cationic porphyrins. *Photochem. Photobiol.* **2002**, *75*, 462–470.
- Oliveros, E.; Bossmann, S.H.; Nonell, S.; Martí, C.; Heit, G.; Tröscher, G.; Neuner, A.; Martínez, C.; Braun, M. Photochemistry of the singlet oxygen [$\text{O}_2(^1\Delta_g)$] sensitizer perinaphthenone (phenalenone) in *N,N'*-dimethylacetamide and 1,4-dioxane. *New J. Chem.* **1999**, *23*, 85–93.
- Redmond, R.W.; Gamlin, J.N. A compilation of singlet oxygen yields from biologically relevant molecules. *Photochem. Photobiol.* **1999**, *70*, 391–475.